PNAS

Supporting Information for

The *Arabidopsis* ORP2A Mediates ER-Autophagosomal Membrane Contact Sites and Regulates PI3P in Plant Autophagy

Hao Ye[1], Jiayang Gao[1], Zizhen Liang[1], Youshun Lin[1], Qianyi Yu[1], Shuxian Huang[1] and Liwen Jiang[1,2,3*]

Corresponding to Liwen Jiang

Email: ljiang@cuhk.edu.hk

This PDF file includes:

Figures S1 to S14
Supplementary Methods
Supplementary References

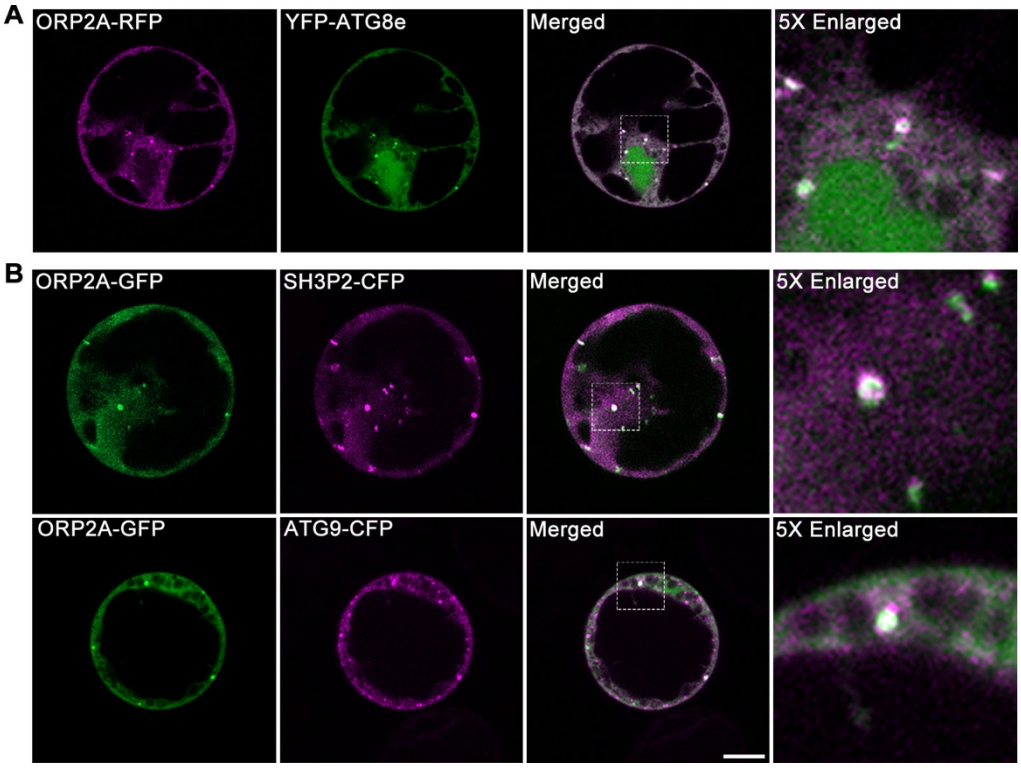

Figure S1. ORP2A colocalizes with autophagy markers upon their transient co-expression in *Arabidopsis* protoplasts.

(A) ORP2A-RFP colocalized with YFP-ATG8e upon their transiently co-expression in *Arabidopsis* protoplasts. Examples of colocalization in the dashed boxes are also shown in the enlargement. Bar = 10 μm.

(B) ORP2A-GFP colocalized with SH3P2-CFP or ATG9-CFP upon their transiently co-expression in *Arabidopsis* protoplasts. Examples of colocalization in the dashed boxes are also shown in the enlargement. Bar = 10 μm.

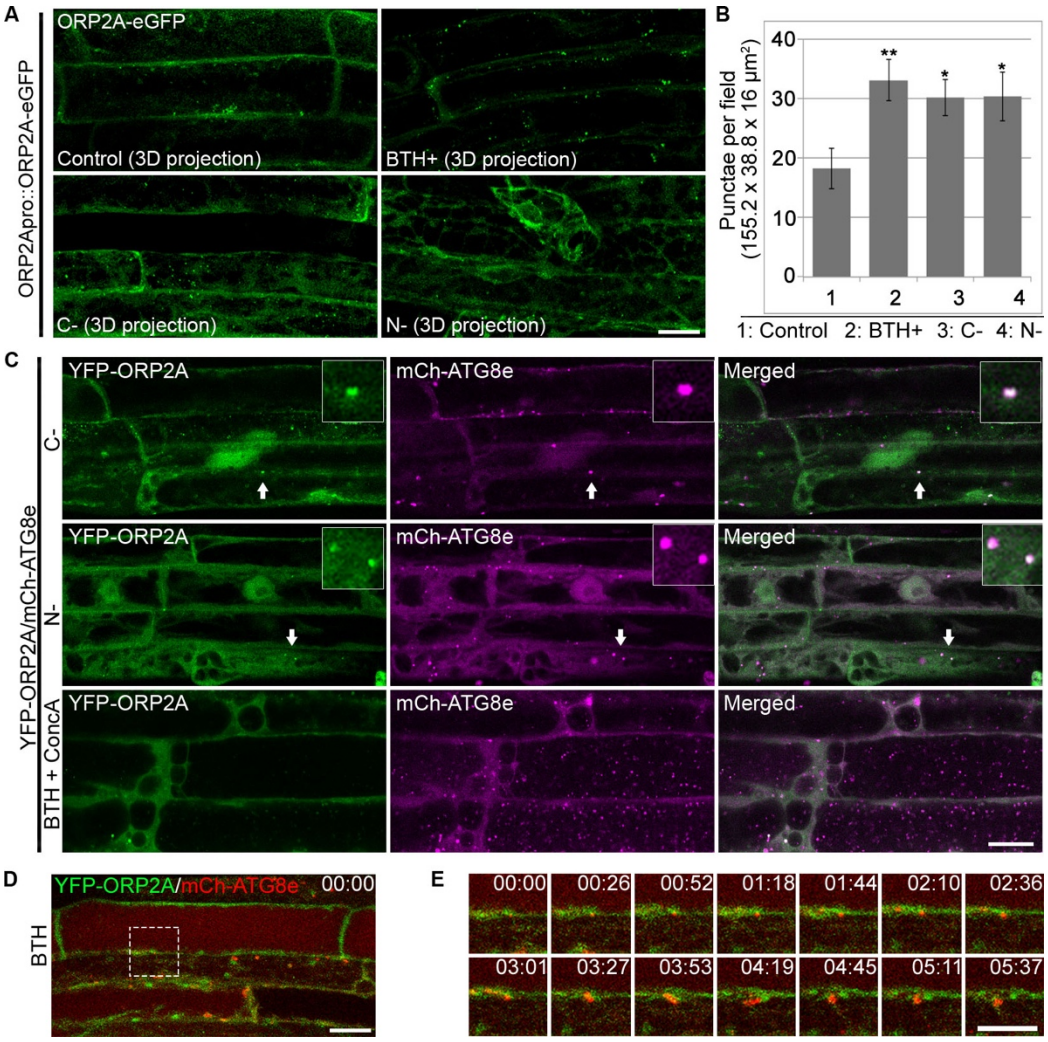

Figure S2. Dynamics of the fluorescent tagged ORP2A-positive punctae in root cells.

(A) Roots of 7-day-old transgenic *Arabidopsis* seedlings expressing ORP2A-GFP under the control of its native promoter (OPR2Apro::ORP2A-eGFP) were subjected to various treatments of MS medium as Control, MS medium with 100 µM BTH for 6 h (BTH), carbon starvation (C-), and nitrogen deletion (N-), followed by confocal imaging and 3D projection. ΔZ = 0.8 µm, 20 stacks. Bar = 10 µm.

(B) Quantification of the numbers of ORP2A-eGFP-positive punctae per root section from various treatments shown in **(A)**. Error bars ± SD; *P≤0.05, **P≤0.005.

(C) YFP-ORP2A punctae colocalized with mCh-ATG8e-positive autophagosomes in the cytosol under carbon starvation (C-) and nitrogen deletion (N-) conditions, but not in the vacuole upon BTH+ConcA treatments. Roots of 7-day-old transgenic *Arabidopsis* seedlings expressing ORP2A-GFP under the control of its native promoter (OPR2Apro::ORP2A-GFP) were subjected to various treatments of MS medium as Control, MS medium with 100 μM BTH for 6 h (BTH), carbon starvation (C-), and nitrogen deletion (N-), followed by confocal imaging and 3D projection. Arrows indicated examples of colocalized punctae and enlargement in the box. Bar = 10 μm. ΔZ = 0.8 μm, 20 stacks. Bar = 10 μm.

(D) and **(E)** Roots of 7-d-old transgenic *Arabidopsis* seedlings co-expressing YFP-ORP2A and mCh-ATG8e were transferred to MS medium with BTH (100 mM) for 6 h, followed by time-lapse confocal imaging analysis. **(C)** A representative image showing the beginning (00:00) frame in which the dashed box indicated an example of autophagosome formation; **(D)** Time-lapse analysis of dynamic relationship between YFP-ORP2A (green) and the autophagosome marker mCh-ATG8e (red) in the dashed box shown in A. See also Supplemental Movie 1 for the full time-lapse series. Bars = 10 μm.

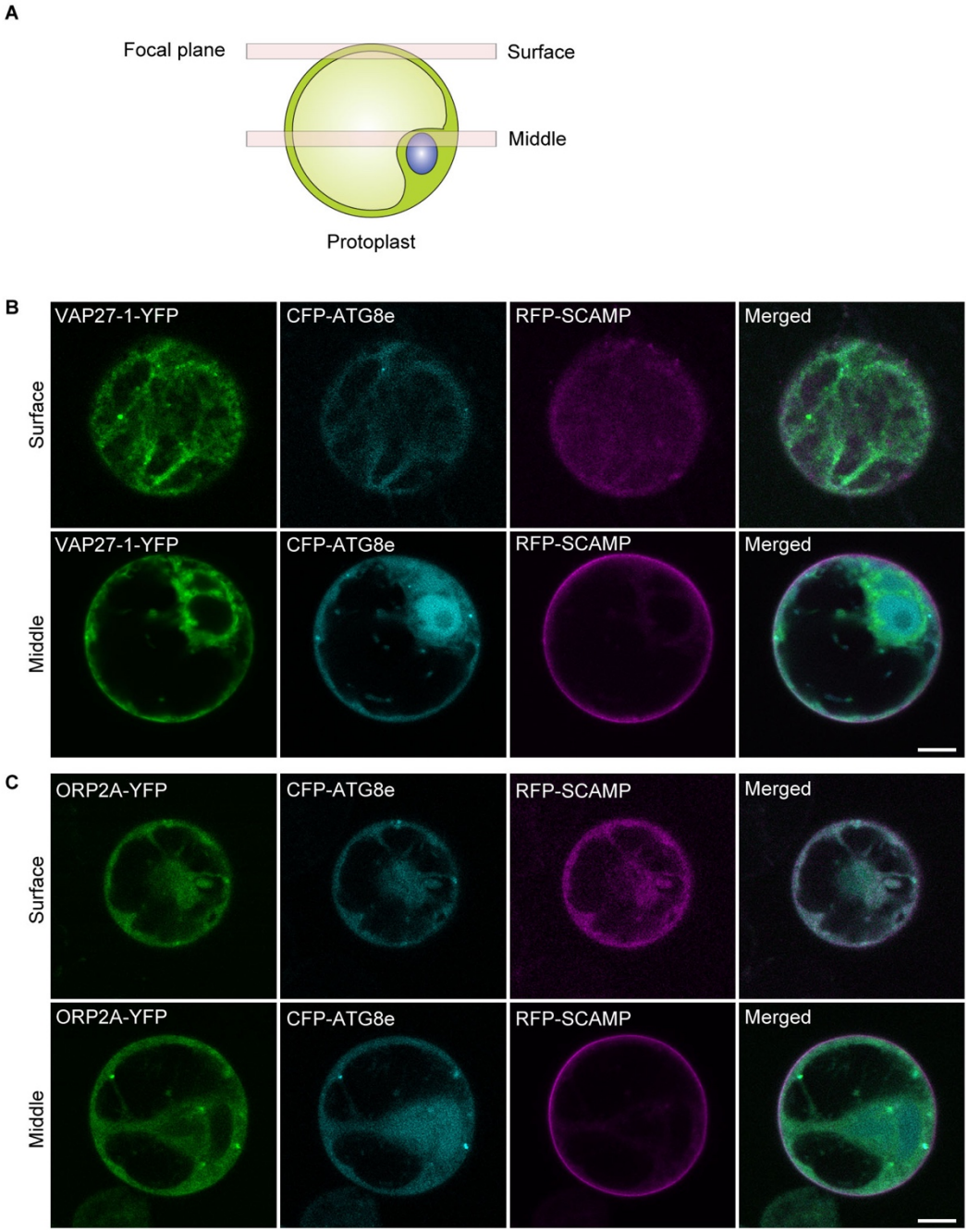

Figure S3. ATG8e colocalizes with ORP2A largely inside the cell but showed less association with the VAP27-1-positive ER-PM contact sites (EPCSs) in the PM region.

(A) Cartoon shows two axial positions of confocal imaging, cell cortex (Surface) and midplane (Middle).

(B) CFP-ATG8e-positive autophagosomes were detected inside the cell and largely distinct from the VAP27-1-RFP-positive EPCSs. *Arabidopsis* PSBD

protoplasts transiently triple-expressing VAP27-1-YFP, CFP-ATG8e and the PM marker RFP-SCAMP together were subjected to confocal imaging at the two focal planes as shown in **(A)**. Bar = 10 μm.

(C) CFP-ATG8e-positive autophagosomes colocalized with ORP2A inside the cell but showed less association with the PM. ORP2A-YFP, CFP-ATG8e and RFP-SCAMP were transiently expressed together in *Arabidopsis* PSBD protoplasts, followed by confocal imaging at the two focal planes as shown in **(A)**. Bar = 10 μm.

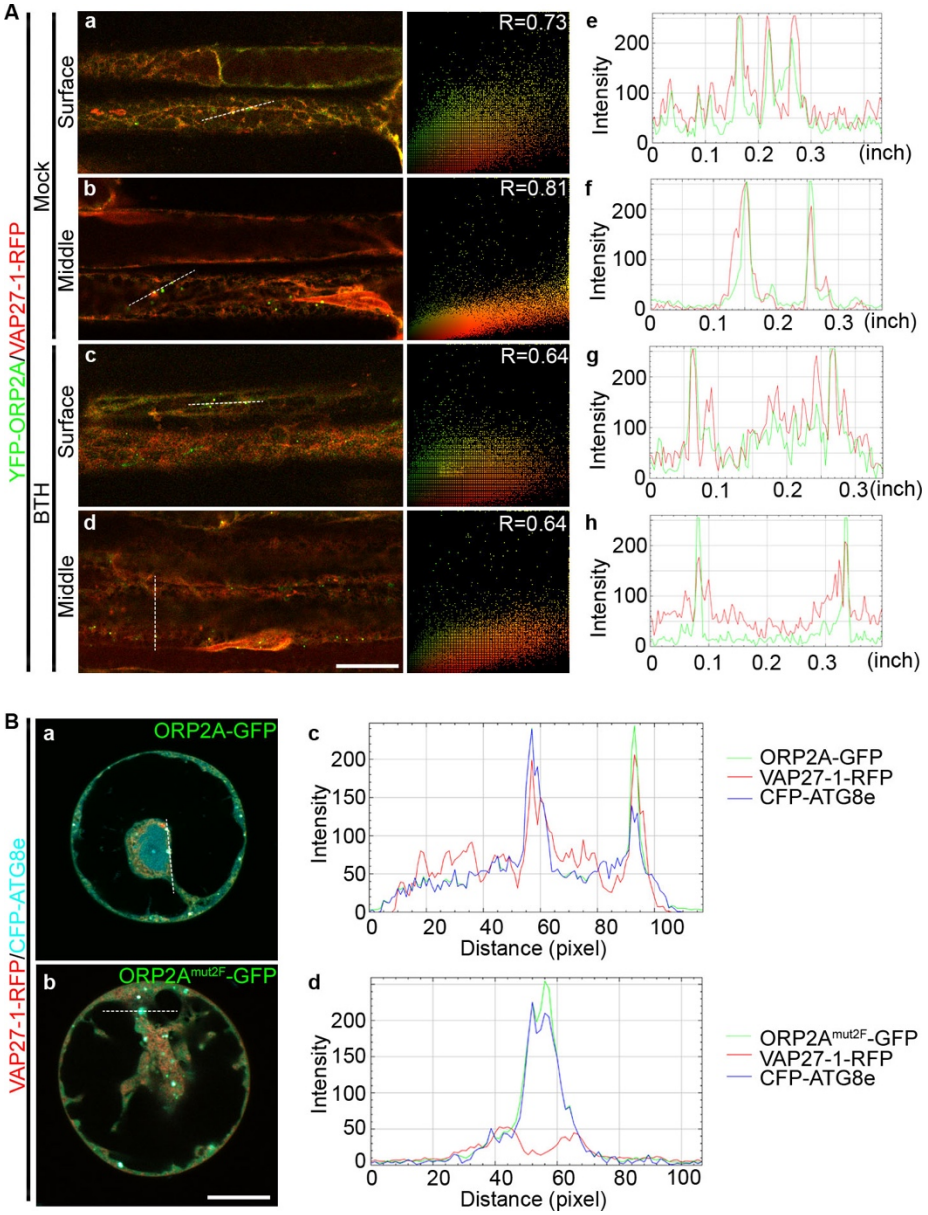

Figure S4. Colocalization analysis of ORP2A and VAP27-1 in transgenic plants and protoplasts.

(A a,b,c and **d)** Pearson correlation coefficient analysis of images in **Figure 2B**. The scatterplot images and the Pearson correlation coefficient (R) obtained from Image-Pro Plus. Bars = 10 μm. **(e, f, g** and **h)** The intensity profiles of the fluorescence signals along the white dashed lines shown in **(a, b, c** and **d)** respectively. The green lines represent ORP2A-GFP signals; the red lines represent VAP27-1-RFP signals.

(B) The intensity profiles of the images in **Figure 2E**. **(c** and **d)** were plotted along the white dashed lines shown in **(a** and **b)** respectively.

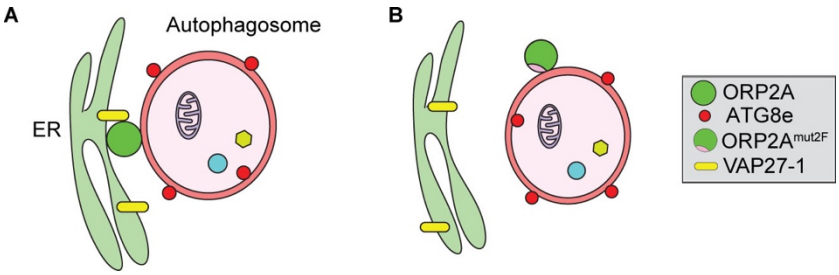

Figure S5. Working model of ORP2A localization and function in autophagy. **(A)** ORP2A localizes on the ER-autophagosomal membrane contact site, bridging together the VAP27-1-positive ER membrane and ATG8e-positive autophagic membrane; **(B)** ORP2Amut2F abolished its interaction with VAP27-1 and thus failed to anchor the ATG8e-labeled autophagosomes to the ER membrane.

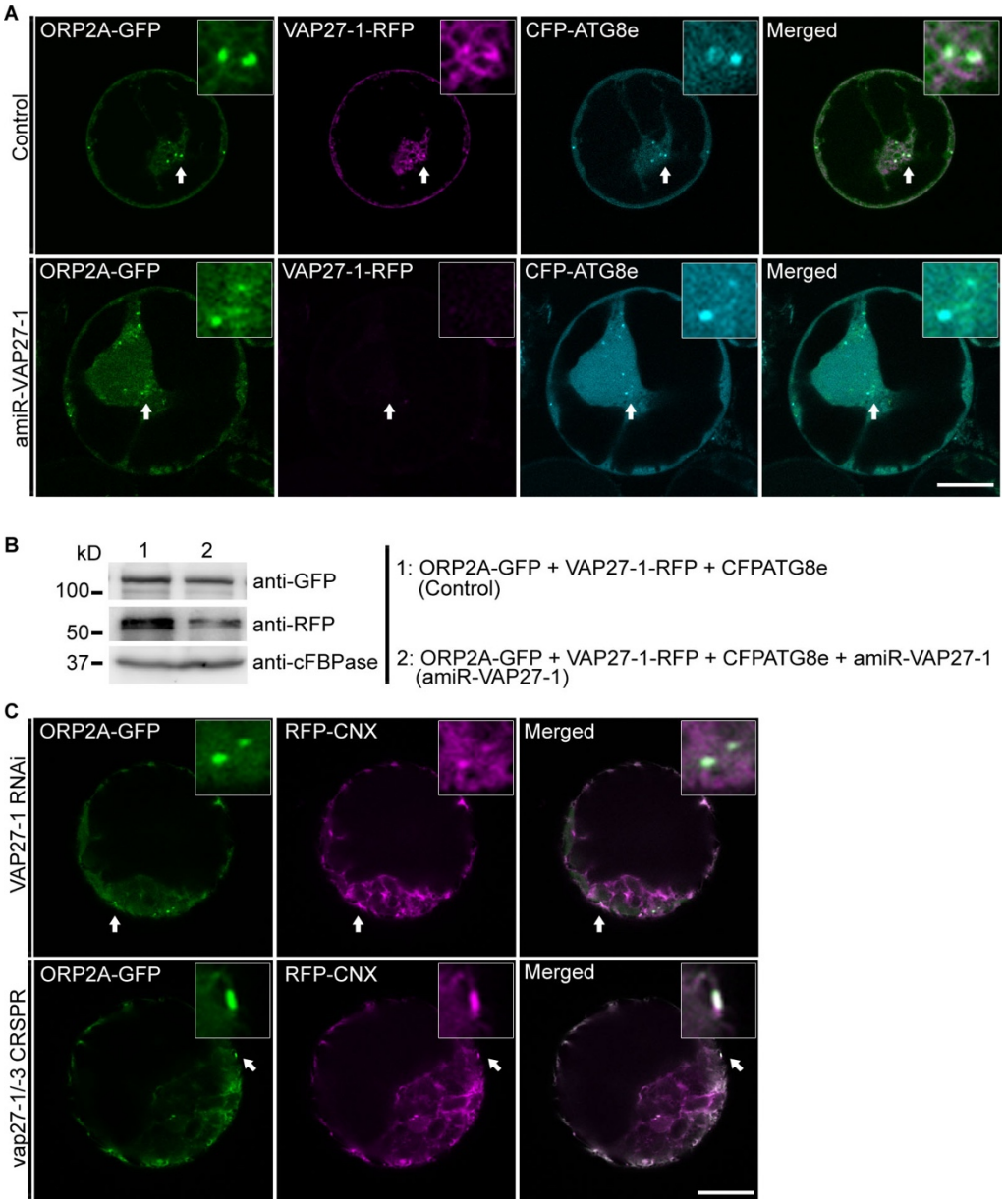

Figure S6. ORP2A colocalized with autophagosome and ER markers in VAP27 KD/KO protoplasts.

(A) ORP2A-GFP, VAP27-1-RFP, CFP-ATG8e were transiently co-expressed together with amiR-VAP27-1 or without amiR-VAP27-1 (control) in *Arabidopsis* protoplasts, followed by confocal imaging analysis. Arrows indicated examples of colocalized punctae and enlargement in the box. Bar = 10 μm.

(B) Total proteins were extracted from cells shown in **(A)**, followed by immunoblot analysis using GFP and RFP antibodies. cFBPase antibodies were used as a loading control.

(C) ORP2A-GFP and RFP-CNX were transiently co-expressed in leaf protoplasts of VAP27-1 RNAi knockdown (KD) plants (top) or *vap27-1/vap27-3* CRISPR knockout (KO) plants (bottom), followed by confocal imaging analysis. Arrows indicated examples of colocalized punctae and enlargement in the box. Bar = 10 μm.

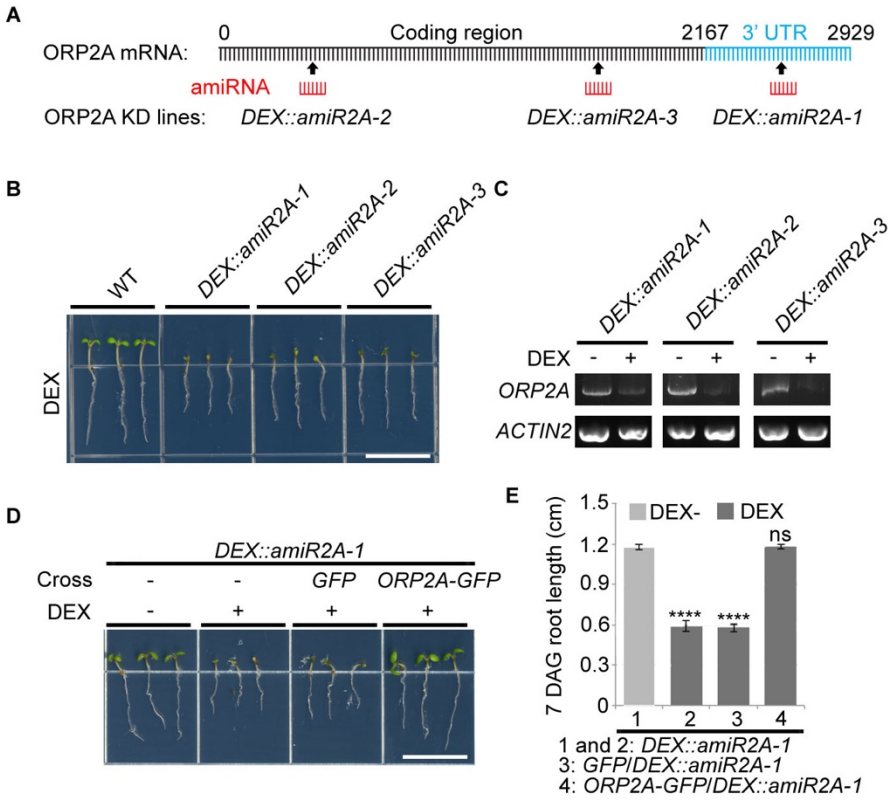

Figure S7. Phenotypic analysis of *DEX::amiR2A* knockdown (KD) plants.

(A) Schematic diagram of ORP2A mRNA and generation of DEX-induced artificial microRNA interference (*amiR*) ORP2A knockdown (KD) lines 1, 2 and 3 (*DEX::amiR2A-1*, *DEX::amiR2A-2* and *DEX::amiR2A-3*). Arrows indicated the *amiR* targeting sites at the indicated positions.

(B) Phenotypic analysis of various *DEX::amiR2A* lines. Seeds from *DEX::amiR2A-1*, *DEX::amiR2A-3* and *DEX::amiR2A-4* lines were geminated and grown on solid MS medium with or without DEX for 7 days, followed by photography. Plates were vertically placed in growth chamber with long-day light period. Bar = 1 cm.

(C) KD efficiency analyzed by reverse transcription PCR (RT-PCR). Seeds from *DEX::amiR2A-1*, *DEX::amiR2A-3* and *DEX::amiR2A-4* lines were geminated and grown on solid MS medium for 5 days and transferred to MS liquid medium with or without DEX for 48 h, followed by RNA extraction and subsequent RT-PCR.

(D) Complementation of the *DEX::amiR2A-1* KD plants with expression of ORP2A-GFP. Seeds of *DEX::amiR2A-1* expressing GFP (control) or ORP2A-

GFP were grown on MS plates with or without DEX as indicated for 7 d, followed by photography. Bar = 1 cm.

(E) Quantification of seedling root length in **(D)**. Error bars ± SD; ****P ≤ 0.0001, student's t-test.

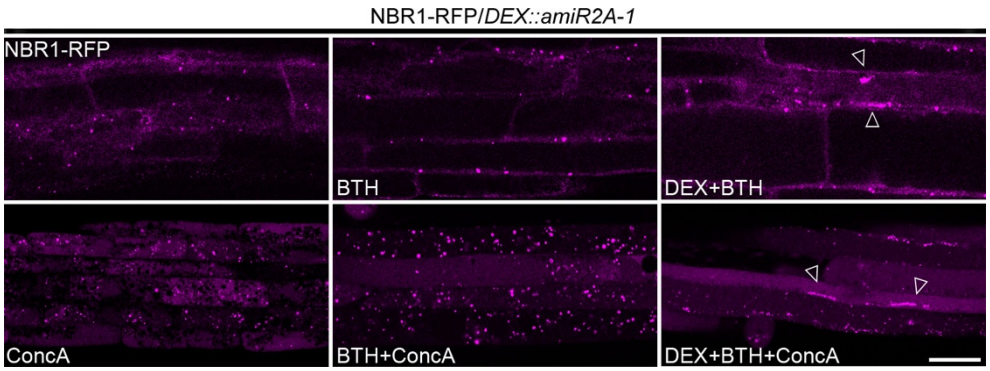

Figure S8. NBR1-RFP accumulated in root cells of ORP2A KD plants.

Root cells of *amiR2A-1* seedlings expressing NBR1-RFP were subjected to various treatments as indicated, followed by confocal imaging analysis. Arrowheads indicated examples of tubular NBR1-RFP signals in the cytosol of ORP2A KD cells (DEX treatments). Bar = 10 μm.

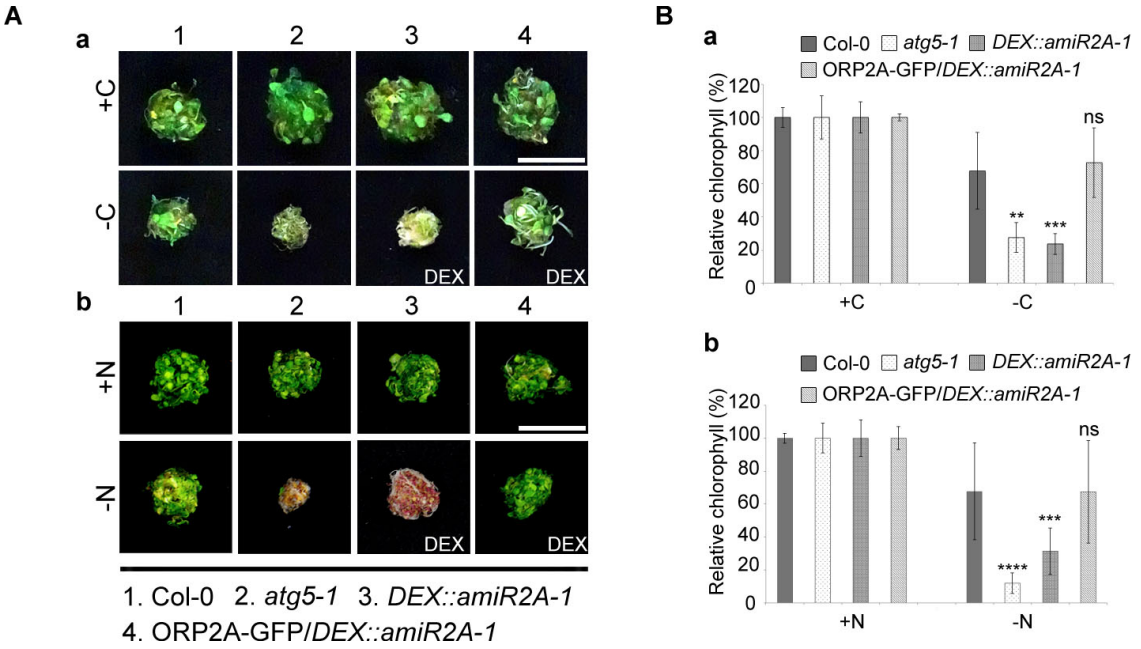

Figure S9. ORP2A KD seedlings display hypersensitivity to nutritional stress.

(A) 7-d-old indicated seedlings grown on 1/2 MS plates with 1% sucrose were subsequently transferred to: **(a)** 1/2 MS liquid medium with sucrose (+C) (control) or without sucrose (–C) for a 7-day constant dark treatment. Seedlings were then recovered under LD for 12 days; **(b)** either nitrogen-containing (+N) or nitrogen-deficient (–N) medium with/without DEX for 4 weeks. Seedlings were then transferred back to +N medium with/without DEX for a 2-week recovery. Bars = 1 cm.

(B) Quantification of the relative chlorophyll contents of indicated seedlings upon carbon starvation **(a)** and nitrogen starvation **(b)**. Error bars ± SD; ns, no significance, **P≤0.005, ***P≤0.001, ****P ≤ 0.0001, student's t-test.

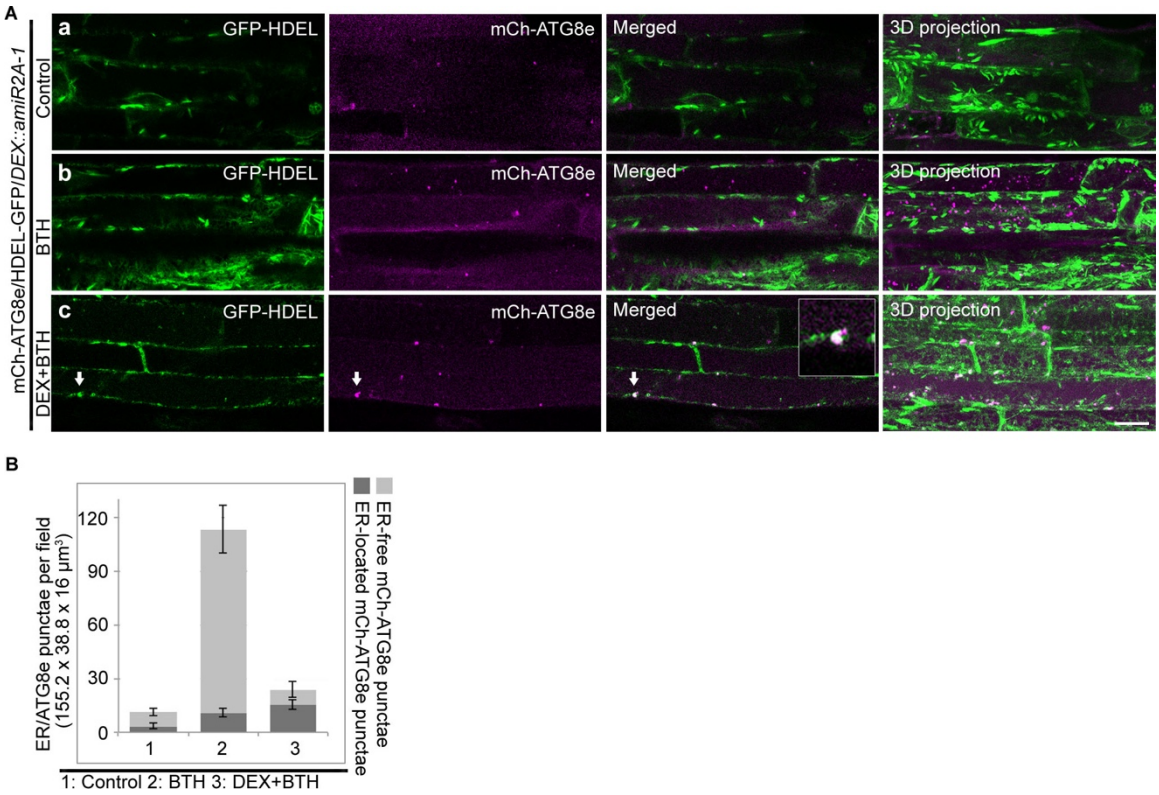

Figure S10. mCh-ATG8e accumulated in and associated with the ER membranes during autophagy in ORP2A KD plants.

(A) 7-d-old transgenic mCh-ATG8e/GFP-HDEL/*DEX::amiR2A-1* seedlings were treated without **(a)** or with BTH (BTH) **(b)** for 6 h, followed by confocal imaging and 3D projection. ΔZ = 0.8 μm, 20 stacks. For DEX+BTH treatment (**c**), DEX pretreatment was performed for 48 h before BTH treatment, followed by confocal imaging and 3D projection. Arrows indicated examples of colocalized dots and the enlargement in the box. Bar = 10 μm.

(B) Quantification of the numbers of ER-free mCh-ATG8e punctae and ER-located mCh-ATG8e punctae (ER/ATG8e) per root section in different treatments shown in **(A)**. Error bars ± SD.

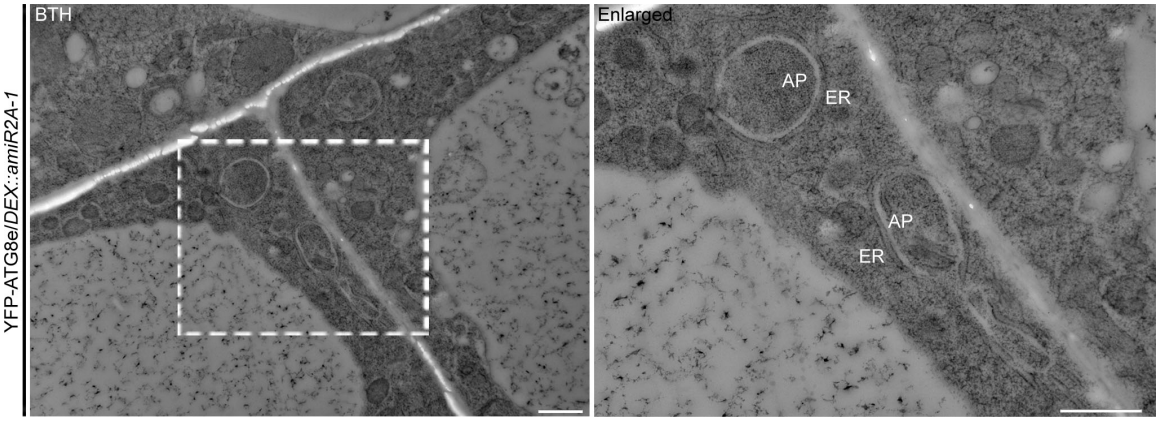

Figure S11. TEM analysis of ER-autophagosomal membrane contact sites in BTH-treated plants.

5-d-old YFP-ATG8e/*amiR2A-1* seedlings were treated with BTH for 6 h, followed by high-pressure freezing/frozen substitution for TEM analysis. The white dashed line box (left) is enlarged (right) to indicate the ER and autophagosomes. AP, autophagosome; ER, endoplasmic reticulum.

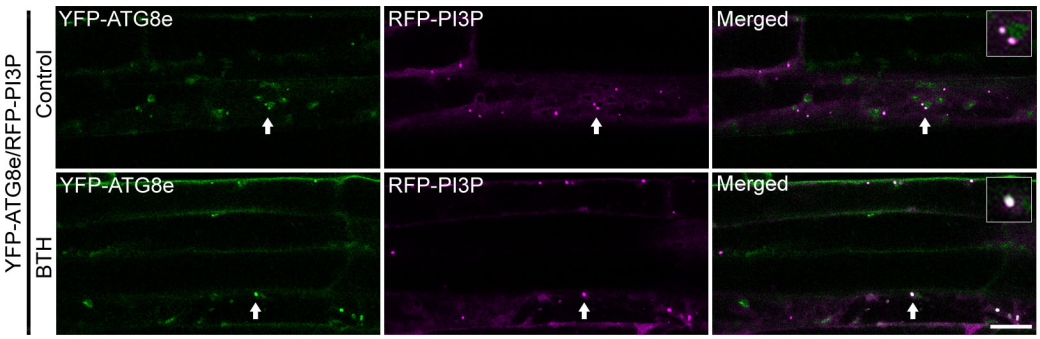

Figure S12. YFP-ATG8e-positive autophagosomes are PI3P-positive in plants.

Root cells of 7-day-old transgenic *Arabidopsis* seedlings co-expressing YFP-ATG8e/RFP-PI3P were treated with (BTH) or without BTH (Control) for 6 h, followed by confocal imaging. Arrows indicated examples of colocalization of these two markers in puncta with corresponding enlargement in the boxes. Bar = 10 μm.

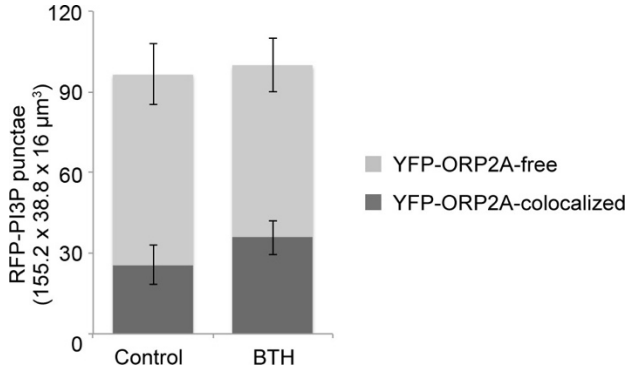

Figure S13. Quantification of colocalization of YFP-ORP2A and RFP-PI3P punctae.

Quantification of the numbers of YFP-ORP2A-free and YFP-ORP2A-colocalized RFP-PI3P punctae per root section shown in **Figure 8A**. Error bars ± SD.

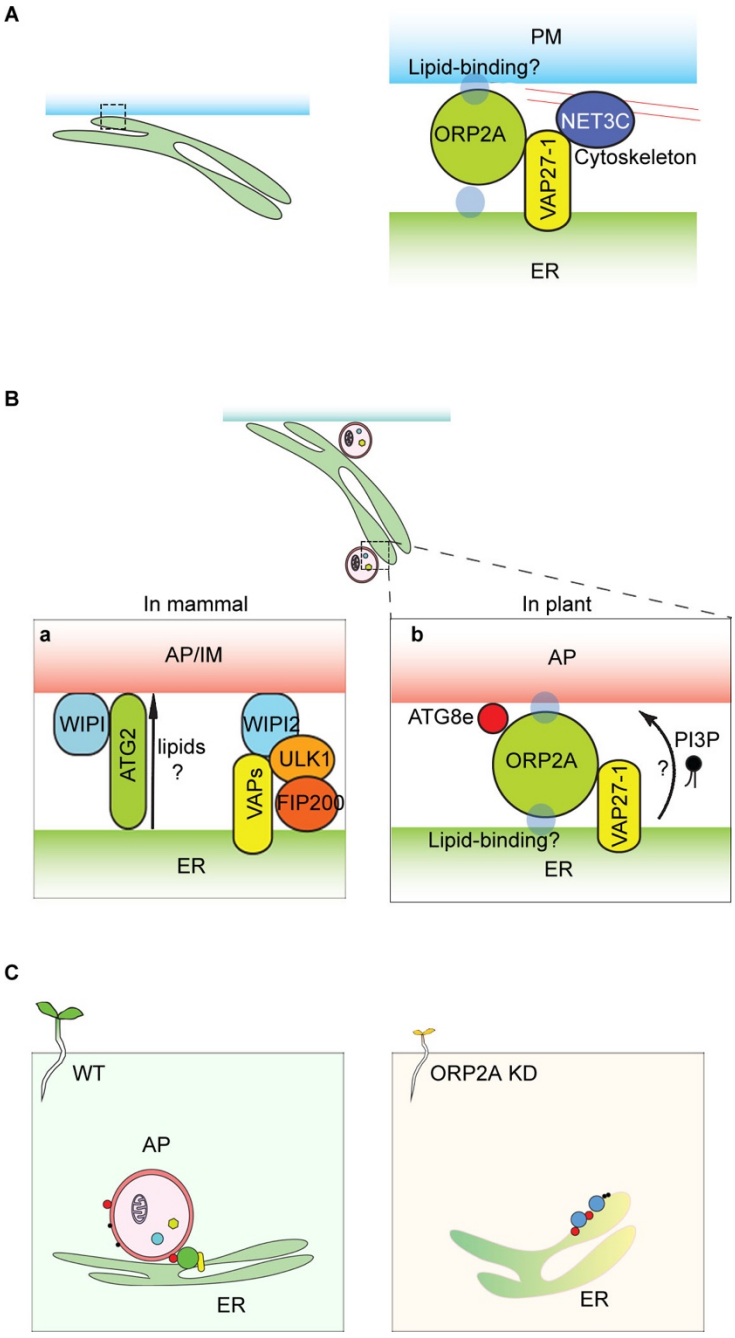

Figure S14. Working models of ORP2A functions in mediating EPCS and EACSs in plants.

(A) Working model of *Arabidopsis* ORP2A function in the EPCS. An EPCS protein complex consists of the VAP27-1, NET3C and the cytoskeleton. The VAP27-1 anchors to the ER membrane through a transmembrane domain and

interacts with the NET3C. The NET3C belongs to the NETWORKED superfamily of actin-binding proteins which forms links between actin filaments and different membrane systems in higher plants. In this study, we propose that ORP2A involves in this EPCS protein complex through direct protein-protein interaction with VAP27-1 and that ORP2A may also bind lipids on the membranes, but its functional role in regulating this architecture remains elusive.

(B) Working models of EACSs in mammal vs. plant.

(a) In mammal, multiple tethering complexes have been identified, which may be diverse in functions at different locations and in different stages of autophagosome biogenesis. In the VAP-mediated EACS, on the ER membrane side, VAPA/B (VAPs) interact with and stabilize the ULK1/FIP200 via FFAT motifs. On the IM side, VAPs interact with the WIPI to mediate the MCS and modulate autophagosome biogenesis. Another linker consisting of ATG2 and WIPI was identified as lipid-transfer protein complex functioning in autophagosome biogenesis. ATG2 was proposed to mediate the EACSs with the PI3P-binding protein WIPI. ATG2 was recently identified as a LTP transferring lipids in bulk between membranes. However, during in vivo lipid transfer, the cargo lipid component and the direction of transfer remain unknown.

(b) In plants, we propose that a protein complex consisting of ATG8e, VAP27-1 and ORP2A mediates the EACS. On one hand, the ORP2A binds to the ER by interacting with the ER membrane protein VAP27-1. On the other hand, ORP2A directly interacts with ATG8e to bind and recruit to the autophagosomal membranes. Lipid-binding may also take part in maintaining the EACSs because ORP2A binds to multiple lipids in membranes. This architecture mediates the EACS and modulates autophagosome formation in plant autophagy. In addition, ORP2A may also function as a LTP channelling the phospholipids (esp. PI3P) from the ER to autophagosmal membranes (or bidirectionally) during autophagosome formation.

(C) ORP2A KD affects plant autophagy and development.

In ORP2A KD plants, autophagosome formation is affected (right). Comparing to the WT (left), ORP2A KD cells exhibited swollen ER with accumulated autophagic proteins and PI3P (right).

AP, autophagosome; ATG, autophagy-related; EACS, ER-autophagosomal membrane contact site; EPCS, ER-PM contact site; ER, endoplasmic reticulum; FFATL, two phenylalanines (FF) in an acidic tract-like; FIP200, FAK family kinase-interacting protein of 200 kDa; IM, isolation membrane; LTP, lipid transfer protein; NET3C, NETWORKED 3C; PI3P, phosphatidylinositol-3-phosphate; PM, plasma membrane; ULK1, Unc-51 like autophagy activating kinase 1; WIPI, WD repeat domain phosphoinositide-interacting protein.

Supplementary Methods

Plant Materials, Growth and Treatment Conditions

Transgenic plants were generated by floral dip (1). Seeds were surface sterilized and sown on Murashige and Skoog (MS) plates with 0.8% agar. The plates were kept at 4°C for 1 d before being transferred to the growth chamber (22°C, 16 h light/8 h dark photoperiod). For starvation treatments, 5-d-old seedlings were grown in liquid MS with methanol (1:100) as mock/control or 100 mM BTH for 6 h prior to observation or as indicated. N starvation was performed by transferring the seedlings to MS or nitrogen-free MS plates for the indicated times. To trigger artificial microRNA expression in *DEX::amiR2A* containing plants, 5-d-old seedlings were transferred to MS liquid medium supplemented with DEX (30 mM) for 48 h before other treatments/observation. In phenotypic analysis of *DEX::amiR2A* plants, seeds were grown on DEX containing plates and imaged as indicated.

Protein Extraction and Immunoprecipitation

Total protein was extracted from 7-d-old seedlings or transformed protoplasts as indicated in the figure legends. Transformed protoplasts were incubated at 26°C for 16 h after transformation. Samples were kept on ice or in 4°C for protein extraction. For protoplasts, cells were collected and washed with 250 mM NaCl solution by centrifugation at 100 x g for 5 min, which were then resuspended in 500 ul lysis/IP buffer (20 mM Tris-HCl pH 7.4, 10 mM MgCl2, 2 mM EGTA, 137 mM NaCl, 0.5% sodium deoxycholate and Complete Protease Inhibitor Cocktail with 0.2% Triton X-100). Resuspended protoplasts were homogenized by passing through a 1 mL syringe with needle for 20 times followed by centrifugation at 10000 × g for 15 min. Supernatants were incubated with GFP-Trap magnetic beads (ChromoTek) and were constantly inverted in a mini tube rotator for 2 h. After incubation, beads were washed for 3 times using ice-cold lysis/IP buffer. Samples were eluted and separated by immunoblot. Antibodies

against SH3P2 and ATG8 were generated and purified as described previously (2).

Chlorophyll Content Measurement

Chlorophyll content was measured using the methods described previously (3). The fresh weights of seedlings were measured before chlorophyll extraction. Samples were immersed in N,N- dimethylformamide and incubated in the dark for 48 h at 4°C. Absorbance was measured by a spectrophotometer at 664 and 647 nm. Total chlorophyll content was calculated and normalized according to sample fresh weight.

Protein Purification and Lipid Binding Assays

Both GST-ORP2A and GST were expressed in *E. coli* Rosetta cells upon induction with 0.5 mM isopropyl β-d-1-thiogalactopyranoside for 20 h at 20°C. Proteins were purified using a GST column in the ÄKTA protein purification system (GE). The lipid binding assay was conduct using the PIP strips/arrays (P-6001/6100; Echelon Biosciences) in room temperature. The strips were blocked in TBST (Tris-buffered saline with Tween: 10 mM Tris-HCl, pH 8.0, 150 mM NaCl, and 0.05% Tween 20) with 1% fat-free milk for 1 h, followed by the incubation with 10 μg/mL of recombinant proteins for 1 h. After incubation, the strips were washed three times in TBS-T and then incubated with GST antibodies for 1 h, then washed by TBST for 3 times. The results were collected in a Chemidoc imaging system (Bio-Rad) following the ECL Plus immunoblot method.

Yeast Two-Hybrid Analysis

MatchMaker GAL4 Two-Hybrid System 3 (Clontech) was used according to the manufacturer's instructions. A pairs of pGBKT7 and pGADT7 vectors (Clontech) were used to carry cDNAs transforming into the Saccharomyces cerevisiae strain AH109. Diploids were selected on synthetic drop-out (SD) medium lacking Trp and Leu (SD-2/+His). Protein interactions were detected by the selection of diploits on SD medium lacking His, Trp, and Leu (SD-3/-His) containing 5 mM 3-AT (3-amino-1,2,4-triazole).

Supplementary References

1. S. J. Clough, A. F. Bent, Floral dip: a simplified method for Agrobacterium‐mediated transformation of Arabidopsis thaliana. *The plant journal* **16**, 735-743 (1998).
2. X. Zhuang *et al.*, A BAR-domain protein SH3P2, which binds to phosphatidylinositol 3-phosphate and ATG8, regulates autophagosome formation in Arabidopsis. *The Plant Cell* **25**, 4596-4615 (2013).
3. S. Xiao *et al.*, Overexpression of Arabidopsis acyl-CoA binding protein ACBP3 promotes starvation-induced and age-dependent leaf senescence. *The Plant Cell* **22**, 1463-1482 (2010).